

DOUBLE-CORE EVOLUTION. III. THE EVOLUTION OF A $5 M_{\odot}$ RED GIANT WITH
A $1 M_{\odot}$ COMPANIONRONALD E. TAAM
Northwestern University

AND

PETER BODENHEIMER
Max-Planck-Institut für Astrophysik and Lick Observatory
Received 1988 May 6; accepted 1988 July 28

ABSTRACT

The two-dimensional axisymmetric evolution of a common envelope configuration consisting of a red giant of $5 M_{\odot}$ and an engulfed main-sequence companion of $1 M_{\odot}$ is calculated. The numerical computations are started at a time when the companion is already deep within the envelope and when hydrodynamic effects first become significant. The results demonstrate that deposition of energy by frictional processes is sufficiently rapid to drive a mass outflow, primarily in the equatorial plane. For the model parameters considered, this result is found to be independent of the evolutionary state of a red giant having a carbon-oxygen core mass in the range of $0.3\text{--}0.8 M_{\odot}$. In all the calculations, most of the material in the common envelope is accelerated to velocities greater than the escape velocity. Several cases are followed to advanced phases when more than $3 M_{\odot}$ of the envelope is ejected. The time scale for mass loss at this stage is typically an order of magnitude shorter than the time scale for spiraling-in of the companion. Thus, the calculations suggest that the entire envelope of the red giant will be ejected, although they do not determine the final orbital separation. The energy efficiency factor, defined as the ratio between the binding energy of the ejected mass and the orbital energy lost by the companion, is estimated to lie in the range $0.3\text{--}0.6$.

Subject headings: stars: binaries — stars: evolution — stars: interiors — stars: late-type

I. INTRODUCTION

The origin of short-period binary systems with a neutron star or white dwarf component is one of the major unsolved problems in the field of binary star evolution. The fundamental difficulty in forming systems such as the low-mass X-ray binary 4U 1820–30 (Verbunt 1987), the binary radio pulsars PSR 1913+16 and PSR 0655+64 (van den Heuvel and Taam 1984), and cataclysmic variables is clear once it is recognized that the progenitors of the compact components must have had a radius much larger than the present-day orbital separation of these systems. In the transformation of long-period binary systems to short-period systems, substantial amounts of mass and angular momentum must have been lost (Ritter 1976). Although evolved stars in the giant region of the H-R diagram lose mass by the action of stellar winds, angular momentum is not lost as effectively. Thus, other mechanisms have been sought in which a torque is applied to the stellar or binary core, whereby angular momentum is transferred to other mass which is subsequently ejected.

One approach which can facilitate the loss of angular momentum in a binary system involves the formation of a common corotating envelope which extends to the outer Lagrangian point. The mass loss through this point leads to a loss of specific angular momentum which is large compared with the specific orbital angular momentum of the system (Nariai and Sugimoto 1976; Flannery and Ulrich 1977; Shu, Lubow, and Anderson 1979). Consequently, the orbital separation continually decreases, resulting in a binary with a short orbital period and a reduced total mass. Another proposed solution to the problem involves the relaxation of the assumption of corotation (Paczynski 1976). Here, the separation of the two stellar cores decreases as a result of the transfer of orbital

angular momentum to the common envelope by frictional and tidal torques. The common envelope is then ejected (carrying with it a large fraction of the initial angular momentum of the binary), either by processes responsible for mass loss in red giants or by the hydrodynamic expansion driven by the high rate of energy deposition generated by friction.

The binary system can evolve into the common envelope stage either if the giant component is not synchronously rotating with the orbital motion at the onset of mass transfer (Counselman 1973) or if the mass transfer process itself is unstable. In the former case, the condition is satisfied when the ratio of the spin moment of inertia of the giant is greater than one-third of the moment of inertia of the binary. For the dimensionless moment of inertia typical of giants ($k^2 \sim 0.2$), synchronism cannot be achieved for mass ratios greater than about 5 or 6. In the latter case, the mass will be transferred on a time scale shorter than the thermal time scale, even approaching the dynamical time scale of the red giant (Paczynski and Sienkiewicz 1972). It is unlikely that the rotation of the giant can maintain synchronism with the orbital motion during these rapid evolutionary phases. Thus, the outcome of tidal evolution in both cases leads to the likely result that the companion plunges into the interior of the red giant.

Since the common envelope phase involves a number of different physical processes operating on a wide range of time scales, the detailed computation of this phase has been largely exploratory in nature. One-dimensional studies have been carried out by Taam, Bodenheimer, and Ostriker (1978), Meyer and Meyer-Hofmeister (1979), Taam (1979), Delgado (1980), Livio and Soker (1984*a, b*), and Soker, Harpaz, and Livio (1984), while multidimensional effects have been investigated by Bodenheimer and Taam (1984, hereafter Paper I) and

recently by Livio and Soker (1988). For an overview of the numerical calculations see the papers by Bodenheimer and Taam (1986) and Taam (1988).

In this paper we focus our attention on the phase of evolution prior to the cataclysmic variable stage and, in particular, investigate the evolution of a $5 M_{\odot}$ red giant with a $1 M_{\odot}$ main-sequence companion. Specifically, we study the late phases of the hydrodynamical evolution of the common envelope phase in two spatial dimensions for a range of initial separations of the double core within the common envelope and for different evolutionary phases of the red giant. In the next section the problem is formulated and the main assumptions underlying the study are given. The detailed results of the numerical computations are presented in § III and discussed in § IV. We summarize our results and make some concluding remarks in § V.

II. FORMULATION

We consider a two-dimensional description of the common envelope of the binary system with the companion located at position R_n . For the region corresponding to the deep interior of the envelope that we consider as our starting point, the assumption that the hydrodynamical flow is axisymmetric is well justified, since the time scale for spiraling in is long compared with the orbital period of the double core. The computations were performed utilizing an explicit Eulerian code and were calculated on a cylindrical grid (R, Z) of 70×70 nonuniformly spaced zones. The detailed numerical technique is described in Black and Bodenheimer (1975), and the differential equations governing the description of the flow are given in Bodenheimer and Taam (1986). Because of the time-step restrictions imposed by the Courant-Friedrichs-Lewy condition on the numerical scheme, the region of the red giant interior to a point just outside the hydrogen and helium-burning shells was not modeled. This region, whose velocity was set equal to zero and whose density and temperature were set constant in time, was treated as a point mass interior to the inner boundary of the envelope. Typically, the grid included about $4 M_{\odot}$ of the envelope.

The description of the energy generated by friction and the decay of the binary orbit is similar to that described in Taam, Bodenheimer, and Ostriker (1978) and Paper I. Here, we have modified the energy dissipation rate to take into account its dependence on the Mach number of the relative flow between the companion and the common envelope (see Shima *et al.* 1985). The energy dissipation rate is given by

$$L_{\text{drag}} = \frac{f\pi}{2} R_a^2 \rho (V_0 - V_e)^3, \quad (1)$$

where the factor f is obtained from interpolation of the results of Shima *et al.* (1985). Here ρ is the local density in the common envelope, and $V_0 - V_e$ is the relative velocity of the companion with respect to the envelope. The accretion radius R_a is modified from the standard form (Hoyle and Lyttleton 1939) to take into account the density variation within it. Specifically, we adopt the form of the accretion radius as determined by Dodd and McCrea (1952), given as

$$R_a = R_0 / [1 + (R_0/2H)^2], \quad (2)$$

where H is the scale height of the density variation in the common envelope and R_0 is the generalized Bondi (1952)

radius estimated as

$$R_0 = 2GM / [(V_0 - V_e)^2 + C^2]. \quad (3)$$

Here M is the mass of the companion and C is the speed of sound in the common envelope at R_n . Note that one can recast equation (2) in the following form:

$$R_a/H = (H/R_0 + R_0/4H)^{-1}.$$

Since R_0 is greater than H , we find that the capture radius is very well approximated by the density scale height in the common envelope. The energy and angular momentum lost from the orbit were distributed over an annular ring with radius equal to R_a (typically corresponding to ~ 5 radial zones).

The early phases of the spiral in process have not been modeled here, since the time scale for orbital decay ($\sim 10^3$ – 10^4 yr; Taam, Bodenheimer, and Ostriker 1978) is much longer than the dynamical time scale which our numerical method can follow. During these phases the red giant can readjust thermally so that hydrostatic equilibrium is maintained (Taam, Bodenheimer, and Ostriker 1978; Taam 1979). Livio and Soker (1988) have recently studied this phase in three dimensions in an exploratory calculation. Although they find that a small fraction of mass can be ejected, their neglect of energy transport by convective motions probably leads to an overestimate of the amount of energy that is transferred into the hydrodynamic mode. It is clear from their calculations, however, that the spiraling-in process must continue to smaller orbital separations. Eventually, the double core spirals to the point where hydrodynamic effects become important, i.e., where the energy deposition is more rapid than the energy transport. It is this phase which is the starting point of the present investigation. Specifically, our initial condition was chosen such that the energy lost in the orbital decay from the red giant surface to the starting point is comparable to the binding energy of the exterior mass. For larger initial separations the main-sequence companion would have to spiral in farther (and hence require more computation time) before significant hydrodynamical motion would develop.

III. NUMERICAL RESULTS

A $5 M_{\odot}$ zero-age main-sequence star of Population I composition ($X = 0.7$, $Y = 0.28$, $Z = 0.02$) was constructed and evolved to the double (hydrogen- and helium-burning) shell source phase with the Eggleton (1971, 1972) stellar evolution code. The models were constructed with account taken of the gravitational potential of a $1 M_{\odot}$ companion situated at position R_n . In these one-dimensional models the added potential was included as an average over a spherical shell. The spherical models were then relaxed to hydrostatic equilibrium on the two-dimensional cylindrical grid with the gravitational potential of the companion now included as an average in an annular ring. As discussed in the previous section, the core region of the red giant was replaced by a point whose mass was chosen such that the relaxation to hydrostatic equilibrium was rapid. The outer boundary of the grid was determined by the radius of the particular evolutionary model and was set at a radius of about 10^{13} cm. The photospheric layers of the red giant, however, are not resolved. The outer boundary condition is taken to be that of a rigid wall until the flow approaches the boundary, after which it is changed to that of a transmitting boundary.

TABLE 1
INITIAL MODEL PARAMETERS

Sequence	M_c (M_\odot)	P_R (days)	R_n (10^{11} cm)	P_r (days)
1.....	0.62	157	4.0	1.4
2.....	0.62	157	4.0	1.4
3.....	0.62	157	6.1	2.6
4.....	0.82	264	4.2	1.7
5.....	0.29	70	5.9	2.1

NOTE.— M_c is the mass of the carbon-oxygen core of the red giant, P_R the orbital period of the initial system, R_n the position where the main-sequence star is initially inserted, and P_r the orbital period of the main-sequence star corresponding to R_n .

Each of the evolutionary sequences is parameterized by the mass of the carbon-oxygen core and the assumed initial location of the main-sequence star. In all models the rotational profile of the envelope is assumed to be one of uniform rotation (see Paper I). The total angular momentum is set equal to that lost by the companion in its spiral from the surface of the red giant to R_n . The initial model parameters for all the sequences are summarized in Table 1.

a) Standard Model: Sequence 1

Since the average mass of white dwarfs in the Galaxy is about $0.6 M_\odot$, we choose as our standard model a red giant with a $0.62 M_\odot$ carbon-oxygen core. The initial binary orbital period before spiraling in is about 0.43 yr (see Table 1), and we take as our initial starting point for the calculation a double-core separation of $5.76 R_\odot$. The local density in the common envelope is $4 \times 10^{-4} \text{ g cm}^{-3}$, resulting in a drag luminosity of about $10^8 L_\odot$. After some initial readjustment, the energy input rate settles to a rate of about $2.5 \times 10^7 L_\odot$ (see Fig. 1).

Because the energy is deposited at such a rapid rate, the energy is not transported efficiently toward the surface by radiative diffusion but, instead, is converted into kinetic energy of motion. The velocity field and density distribution in the grid at time 0.07 yr are shown in Figure 2. It can be clearly seen that the matter is primarily driven outward at velocities $\sim 100\text{--}200 \text{ km s}^{-1}$ in the equatorial plane in a manner similar to that described in Paper I. As a consequence of this material flow, a counterclockwise circulation develops in the core region. It should be noted that at this time the flow for R greater than 5×10^{12} cm is moving at about 20 km s^{-1} and is more nearly spherical. The angular momentum lost from the binary orbit is primarily redistributed in the radial direction by the matter outflow, leading to only a slight spin-up of the common envelope near the vicinity of the companion star. This is shown in Figure 3, where the ratio of the envelope velocity to the orbital velocity of the companion is plotted as a function of time. It can be seen that in the initial phases the ratio increases from 0.12 to a maximum of 0.27, after which the ratio reaches a temporary plateau phase. As the evolution proceeds, the matter in the equatorial regions accelerates to higher velocities, so at time 0.1 yr the velocities are supersonic. At this time the high-velocity matter is moving at $\sim 300 \text{ km s}^{-1}$, which is greater than the escape speed, and is concentrated to the plane, with mass loss occurring over a half-angle of $\sim 12^\circ$ (see Fig. 4). Because of the high outflow velocity the local envelope velocity decreases (see Fig. 3) as the angular momentum lost from the orbit is efficiently advected outward. This phase corresponds to the onset of mass loss; most of the matter is moving at velocities less than that required for escape (see Fig. 5). However, at time 0.14 yr the mass-loss process accelerates to a rate of over $160 M_\odot \text{ yr}^{-1}$. As can be seen in Figure 5, the amount of mass moving outward decreases, reflecting the loss of about $3.2 M_\odot$ from the common envelope. As a result of the reduction in density in the envelope, the mass-loss rate declines

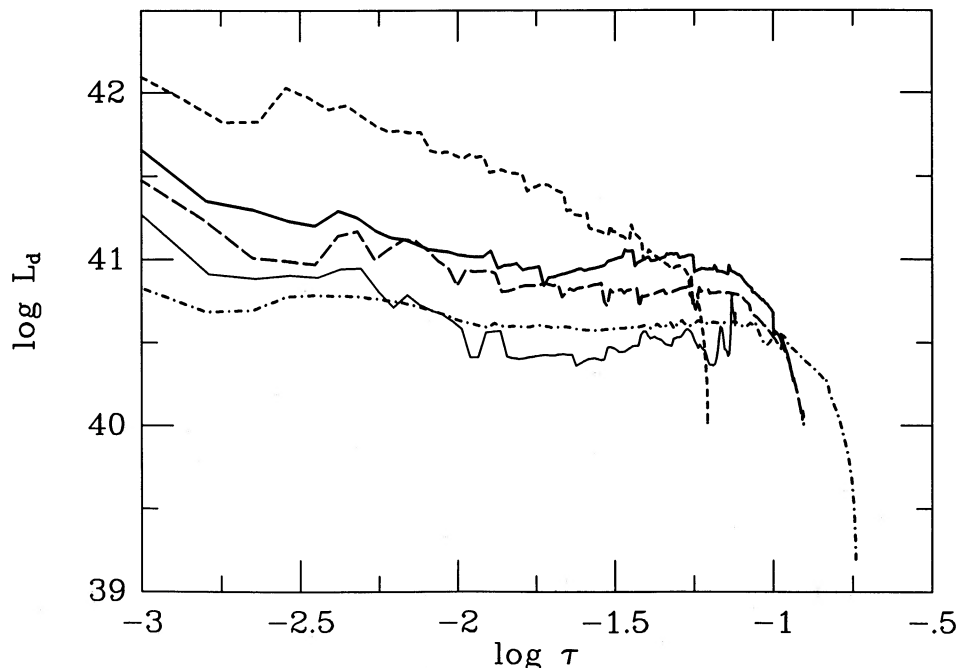


FIG. 1.—Energy dissipation rate as a function of time in years for all the evolutionary sequences. Sequences 1, 2, 3, 4, and 5 are denoted by the heavy solid, dot-dash, long-dashed, light solid, and short-dashed curves, respectively.

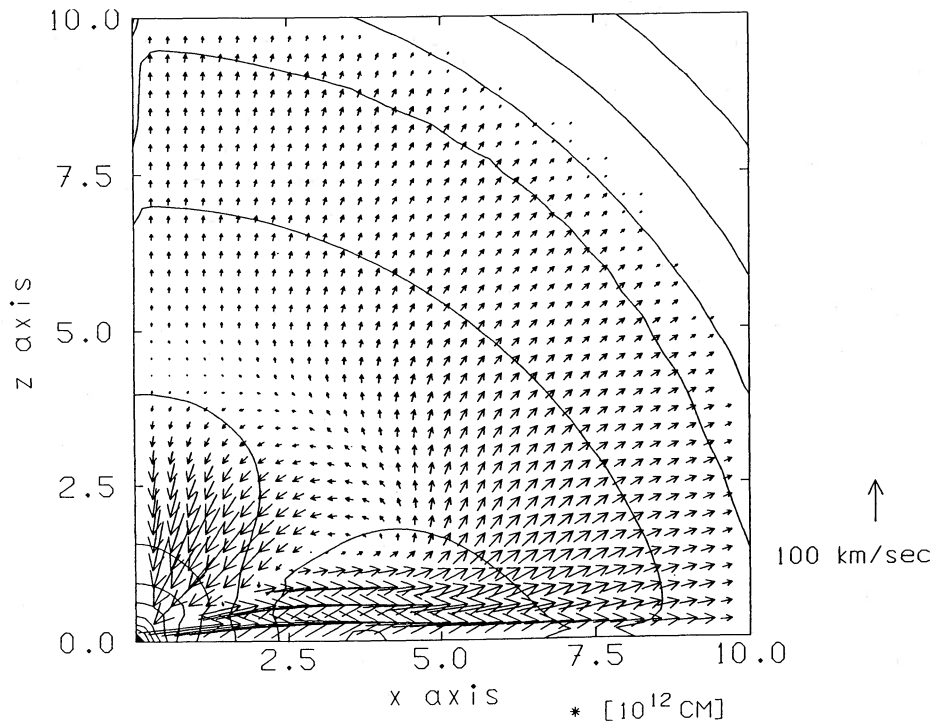


FIG. 2.—Velocity field and density distribution of sequence 1 at time 0.07 yr in the common envelope. The maximum velocity in the grid is 266 km s^{-1} , and the 12 density contours are spaced logarithmically ranging from $\log \rho = -6.9$ to $\log \rho = -3.6$.

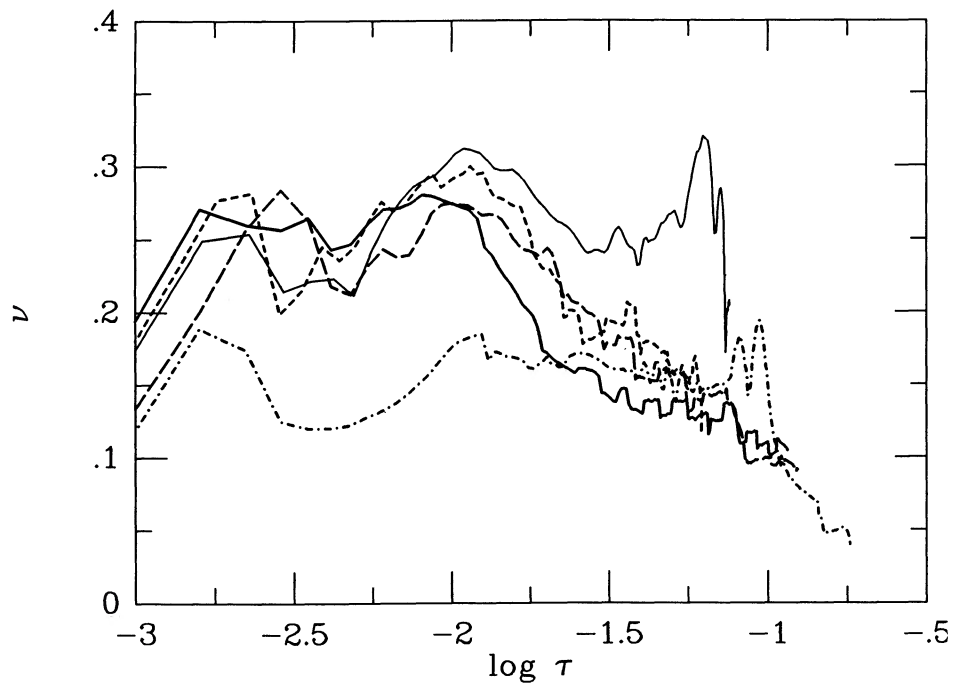


FIG. 3.—Ratio of the envelope velocity at R_e (in units of 10^{10} cm) to the orbital velocity of the companion. The sequences are distinguished according to the pattern given in Fig. 1.

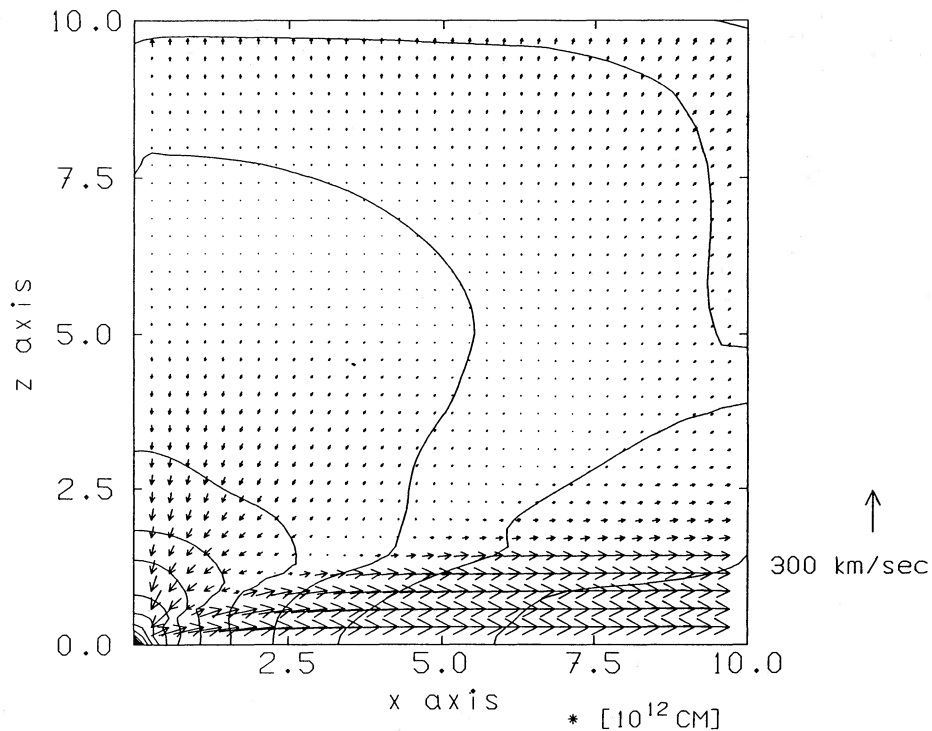


FIG. 4.—Velocity field and density distribution of sequence 1 at time 0.1 yr in the common envelope. The maximum velocity in the grid is 340 km s^{-1} , and the 11 density contours are spaced logarithmically ranging from $\log \rho = -6.6$ to $\log \rho = -3.6$. The matter within 12° of the equator is moving at velocities approaching the escape velocity from the double core.

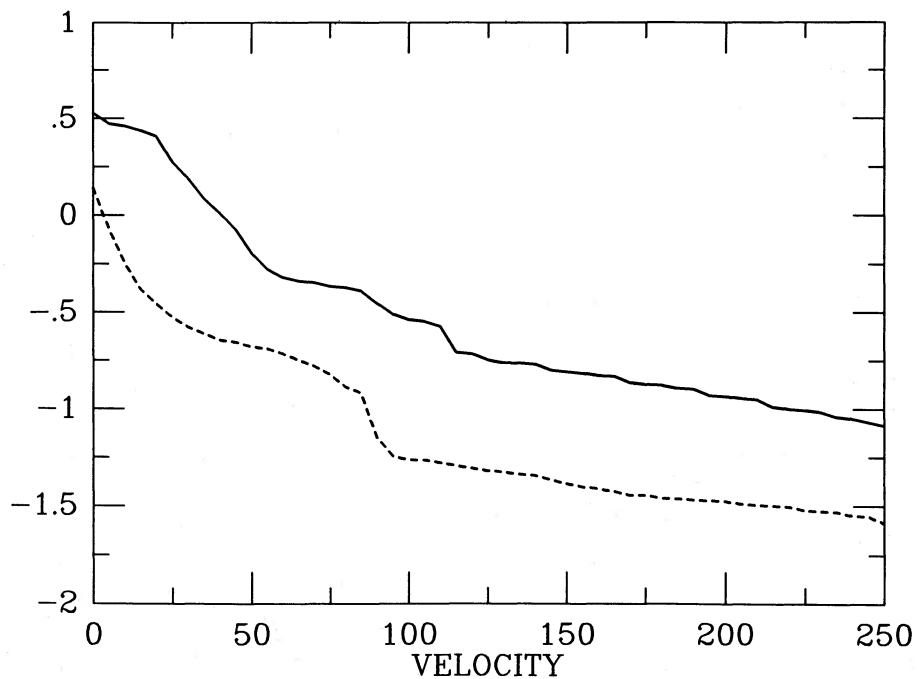


FIG. 5.—Mass in M_\odot in the common envelope moving with velocities > 0 , in units of km s^{-1} , are shown at two different times for sequence 1. Time 0.1 yr is denoted as a solid line, and time 0.14 yr is denoted by the dashed line.

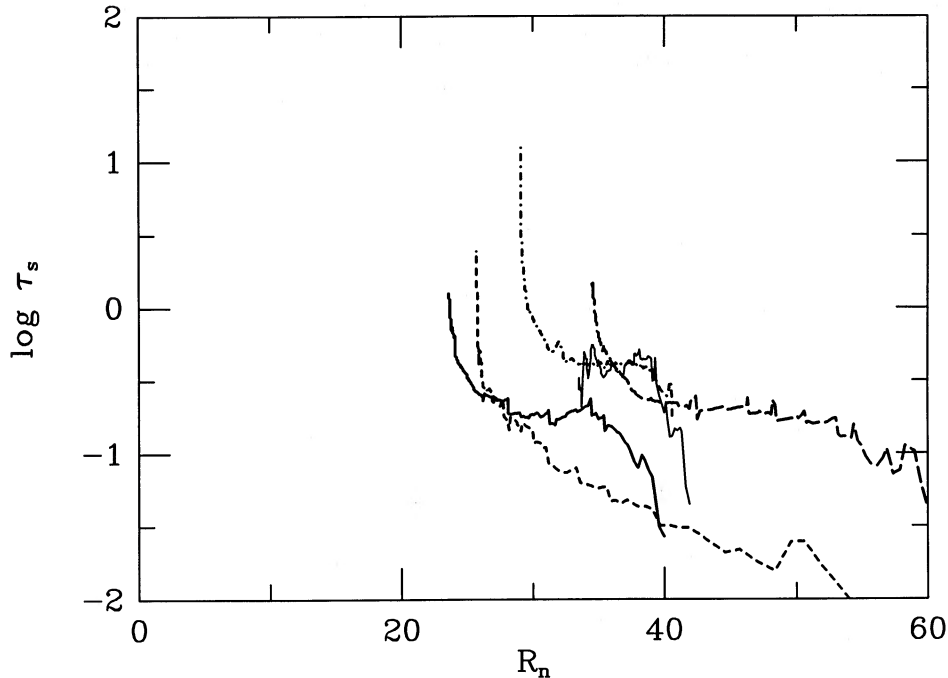


FIG. 6.—Orbital decay time scale (in years) as a function of the position of the companion (in units of 10^{10} cm) for the five evolutionary sequences. The sequences are coded as in Fig. 1. Note that toward the latter evolutionary phases of the sequences the orbital decay time scale rapidly increases.

to about $30 M_{\odot} \text{ yr}^{-1}$. At this point the density in the vicinity of the companion has declined sufficiently (by more than an order of magnitude to $2 \times 10^{-5} \text{ g cm}^{-3}$) that the drag luminosity drops (see Fig. 1) and the spiraling-in time scale increases rapidly (see Fig. 6). By this time the companion has spiraled in to about $3 R_{\odot}$, and the calculations become inaccurate because the energy deposition in the accretion radius begins to influence the inner boundary. In actual fact, the matter within our boundary should begin to flow out to resupply the ejected matter. Consequently we terminated our calculations at this point. The result of the calculations are summarized in Table 2. We remark at this point that the spiraling-in time scale is more than 14 times the mass-loss time scale and that more than 75% of the mass of the common envelope has been ejected. If these results can be extrapolated, it seems likely that the entire envelope will be ejected and that the spiraling-in process will stop.

b) Sequence 2

To determine the sensitivity of the evolution to the form of the energy dissipation rate, we considered a case where the form of the dissipation rate was similar to that given in Paper I. In particular, we neglected the dependence of the drag luminosity on the Mach number of the relative flow (between the companion and the common envelope) and assumed that the accretion radius was constant (equal to 10^{11} cm). We point out that in the previous case the effect of the Mach number dependence on the drag luminosity was not large, since the Mach number was near unity, varying by less than 25%. The initial model parameters were chosen to be identical to those of sequence 1 (see Table 1).

The main difference in the evolution of the double core can be traced to the reduction in the drag luminosity resulting from the smaller accretion radius (by a factor of 2.7 during the initial phase and a factor of 1.4 during the terminal phase of

evolution). In Figure 1 it is seen that the energy dissipation rate is about a factor of 3 smaller than that found in sequence 1 (except during the initial readjustment phase) and is nearly constant at about $1.3 \times 10^7 L_{\odot}$ throughout the main phase of evolution. The basic features of the evolution in this sequence are very similar to those outlined above for sequence 1. However, the temporal evolution progresses more slowly, since the time required to accelerate matter to escape velocity is increased. Consequently, the outflow velocities are lower by about 25% and the ejected matter is confined more to the equatorial plane (within a half-angle of $\sim 7^{\circ}$). At the final stages of the calculation the energy lost from the binary orbit led to the ejection of about $3 M_{\odot}$. During this phase of the evolution the orbital decay time was increasing rapidly with the evolution and exceeded 12 yr when the calculations were discontinued. This is to be compared with a mass-loss time scale of 0.03 yr. We note that the spiraling-in time scale is about an order of magnitude longer than in the standard case, even though the companion has not spiraled in as far. This indicates that the efficiency for conversion of orbital energy

TABLE 2
MODEL RESULTS

Sequence	P_f (days)	R_f (10^{11} cm)	T_m (yr)	T_s (yr)
1.....	0.67	2.36	0.09	1.28
2.....	0.91	2.91	0.03	12.45
3.....	1.18	3.45	0.13	1.52
4.....	1.26	3.35	0.11	0.33
5.....	0.70	2.57	0.03	2.44

NOTE.— P_f is the orbital period at the point where the calculations were terminated, and R_f is the position of the main-sequence star corresponding to orbital period P_f ; T_m and T_s are the mass-loss time scale and the spiraling-in time scale at this point.

into mass ejection in this sequence is somewhat higher. The final parameters of the common envelope evolution are given in Table 2.

c) Sequence 3

Here we increased the separation of the double core to $R_n = 8.78 R_\odot$. The dependence of the accretion radius on the density scale height and the dependence of the drag luminosity on the Mach number of the relative flow were included. Because the companion was placed at a larger radius, the orbital velocity of the companion and the local density were reduced ($\rho \sim 2 \times 10^{-4} \text{ g cm}^{-3}$). On the other hand, since the density scale heights characteristic of the common envelope were larger (by about 50%), the accretion radius increased. As shown in Figure 1, the drag luminosity throughout the evolution is smaller than in sequence 1, but only by a factor of less than 1.6. Consequently, the results of the common envelope calculation are more quantitatively similar to sequence 1 than to sequence 2. In this case, the mass is lost at a smaller rate ($\sim 15 M_\odot \text{ yr}^{-1}$, about a factor of 2 smaller than in sequence 1), corresponding to a mass-loss time scale of 0.13 yr in comparison with the spiraling-in time scale equal to 1.5 yr. Thus, the result that the entire common envelope is likely to be ejected does not depend sensitively on our particular choice of the initial placement of the companion star within the common envelope.

d) Sequence 4

In this sequence the details of the common envelope evolution are investigated for a different evolutionary state of the red giant primary. For a more evolved phase the radius of the red giant is larger and, hence, the binding energy of the common envelope decreases. Thus, it is expected that the envelope would be easier to eject. Accordingly, we have considered a more evolved model with a $0.82 M_\odot$ carbon-oxygen core and, for purposes of comparison, an initial double core separation of $6 R_\odot$. In this case, the energy dissipation rate is lower than in the standard sequence. This is a direct result of the fact that there is less mass interior to the companion position R_n and, hence, (1) the local density in the envelope is lower ($1.75 \times 10^{-4} \text{ g cm}^{-3}$) and (2) the orbital velocity of the main-sequence star is reduced. In fact, $1.02 M_\odot$ lies within $4.2 \times 10^{11} \text{ cm}$, whereas in sequence 1 the mass interior to this point is $1.29 M_\odot$. This latter effect also leads to a smaller Mach number for the motion of the main-sequence star with respect to the common envelope, and thus the orbital energy is deposited more slowly than in either sequence 1 or sequence 3 (see Fig. 1).

The evolution proceeds in a manner similar to the previous cases; however, the evolution could be followed only to the point where the companion star spiraled to $4.8 R_\odot$. At this time little mass has been lost ($\sim 0.1 M_\odot$). The mass-loss rate, however, had already accelerated to about $36 M_\odot \text{ yr}^{-1}$, corresponding to a mass-loss time scale of 0.1 yr. This compares with an orbital decay time of 0.3 yr. At this point the accretion radius equaled $4 R_\odot$, leading to the situation that the energy lost from the orbit was deposited in almost the entire core region. We note that there is only $0.14 M_\odot$ in the grid interior to a spherical radius equal to R_n (excluding the point mass in the center). The overall results, however, closely resemble the evolution of sequence 2 with $R_n = 10^{11} \text{ cm}$. The drag luminosities in both cases are very similar, and when the evolutions are compared at the same double-core separation, they are also very similar. In fact, the mass-loss rate, mass-loss time scale, and spiraling-in time scale for sequence 2 at this point are 33

$M_\odot \text{ yr}^{-1}$, 0.1 yr, and 0.4 yr, respectively. Based upon the results of sequence 2, it is likely that the mass will be ejected much in the same manner as in sequence 2.

e) Sequence 5

Sequence 5 is characterized by a less evolved red giant than in any of the previous sequences. In this case the common envelope is more tightly bound, and we wish to determine whether the results found in the other sequences are applicable to a wider range of parameters. Accordingly, we considered a model for which the CO core is $0.29 M_\odot$. For this model the hydrogen-helium interface lies at a mass equal to $1.2 M_\odot$. In this case we chose an initial double-core separation of $8.5 R_\odot$. The mass lying interior to the companion was $1.85 M_\odot$. With these initial parameters a larger orbital velocity, a larger Mach number for the relative flow, and a higher local density ($7 \times 10^{-4} \text{ g cm}^{-3}$) result, as compared with the standard case. Consequently, the energy input rate by frictional dissipation for sequence 5 is the highest for any of the sequences (see Fig. 1). The evolution is similar to that described for the other cases, but faster (less than 0.1 yr). We remark at this point that during the initial phases of the spiraling in the decay time scale is only about twice as long as the orbital period (see Fig. 6). Hence, the three-dimensional effects investigated by Livio and Soker (1988) may be expected to be important. However, the phase where the decay time scale is comparable to the orbital period of the double core lasts for only about a day, so these effects on the overall common envelope evolution should be minimal. The calculations were continued until the companion spiraled to a separation of $3.7 R_\odot$. At this point, $3.5 M_\odot$ of matter has been ejected within a half-angle of 13° from the equatorial plane at a rate of $64 M_\odot \text{ yr}^{-1}$. The time scale for the ejection of matter above the hydrogen-helium interface is 0.03 yr, compared with a spiraling-in time scale of 2.44 yr (see Table 2).

IV. DISCUSSION

The numerical results of the two-dimensional hydrodynamical simulations indicate that the entire common envelope of the double-core configuration consisting of a $5 M_\odot$ red giant and a $1 M_\odot$ main-sequence companion can be ejected. These results are, furthermore, not sensitive to our particular choice of the initial location of the companion star within the common envelope or to the evolutionary state of the red giant in its double shell burning stage. We remark that although mass motions could start at larger double-core separations, the hydrodynamic ejection of the envelope occurs during the phase which we calculate, since the energy released from the orbit to our initial starting points is insufficient to unbind the overlying layers (see § II). We have also demonstrated that the mass-loss time scale from the common envelope becomes significantly less than the orbital decay time scale during the late phases of evolution. Although we have not been able to follow the evolution to the point where the common envelope phase terminates, the results suggest that the envelope will be ejected before the two cores coalesce. The actual point at which the spiraling-in phase stops has not been modeled, and the manner in which it takes place probably is determined by the behavior of the nuclear burning shells of the red giant. If the circulation induced in the inner regions by the two-dimensional nature of the outflow extends into the burning regions, hydrogen-rich matter may be mixed into the helium-burning region and carbon nuclei from the helium-rich region may be mixed into the hydrogen-burning shell. This would lead to an enhanced energy generation rate in the nuclear burning shells which may

significantly aid in the ejection of matter during the terminal stage. If, on the other hand, the circulations do not penetrate to the burning regions, the extensive mass loss will eventually cause the nuclear burning to be extinguished. In addition, once the mass above the white dwarf core is reduced below some critical value ($<0.001\text{--}0.01 M_{\odot}$), the radius of the primary remnant will then shrink (since the pressures at the base of the burning shells will not be able to support the weight of the overlying matter) and the common envelope phase is expected to terminate.

As noted in Paper I, the ejection process is nearly adiabatic, since the time scale on which energy is deposited into the common envelope is much shorter than the energy transport time scale by either radiation or convection. Thus, most of the orbital energy is converted into the kinetic and potential energy of the outflowing matter. However, the energy is distributed not uniformly over the common envelope but primarily in the equatorial plane. Specifically, the results of our calculations indicate that the mass which lies within or circulates into the region within a half-angle of about 13° from the equatorial plane can be ejected with velocities greater than escape. We note that the mass is ejected over a greater half-angle in the present work than in Paper I. We attribute this difference to the effect of the added potential, which tends to make the density gradients in the vicinity of the secondary more spherical (so that the outflow is not as concentrated toward the equator). Note also that in sequence 2 the outflow angle was confined to 7° , indicating that the size of the accretion radius, which forms essentially the only difference between the parameters of sequences 1 and 2, has a significant effect. As a measure of the efficiency of energy deposition into mass ejection, we use the quantity α defined as the ratio of the binding energy of the mass ejected to the energy released in the orbit (see Iben and Tutukov 1984; Livio and Soker 1988). Although the entire common envelope was not completely ejected in our simulations, the results should give a good indication of the range for α . For the evolutionary sequences which were followed to the late stages of the double-core phase the values of α were found to be about 0.3, 0.4, and 0.6 for sequences 1 and 2, 3, and 5, respectively.

Although the above results suggest that the efficiency for conversion of orbital energy to mass ejection may be higher for less evolved configurations, this is somewhat misleading because of our neglect of the ionization zones in the outer layers of the red giant. In particular, for a sufficiently evolved red giant a portion of the envelope is characterized by positive energies because of the contribution of the helium and hydrogen ionization energy. If this energy can be tapped without significant losses to nonadiabatic effects, then there would be additional energy to drive off the envelope. That is, as the matter is ejected, it cools and recombines, thus providing more energy to enhance the outburst. Thus, a smaller amount of energy from the orbit may be required to eject the entire envelope than is indicated by our calculations. In addition to reducing the energy requirements for mass ejection, the efficient conversion of ionization energy to kinetic energy may facilitate the ejection of matter situated away from the equatorial regions. Thus, its effect may also promote the ejection of the envelope over a more extensive region.

Our calculations also indicate that about $0.1 M_{\odot}$ is accreted by the main-sequence star during the hydrodynamic phase of the common evolution. Since this phase only lasts less than ~ 0.2 yr, the total amount accreted depends upon the hydrostatic phases of common envelope evolution during which the

binary orbit decays from the red giant surface. However, we remark that our result must be regarded as preliminary, since the amount accreted depends on the structural response of the companion (which has not been calculated) to the conditions within the common envelope. This is made evident by the work by Kato (1982) on the structure of a $1 M_{\odot}$ star immersed within a supermassive star, which indicates that both accretion and evaporation are possible. For the accretion rates inferred from the calculations one might expect that the secondary will expand (see Webbink 1976, 1977) to affect the flow. However, if we can define the boundary between the secondary and the common envelope by the critical Roche lobe (see Kato 1982), the degree of expansion will be limited by the size of the lobe. The resulting accretion rate will then be determined by the amount necessary to maintain the secondary in contact with its lobe. Since the lobe is not much larger than the stellar radius, one does not expect the flow to be significantly affected.

V. CONCLUSIONS

The two-dimensional hydrodynamical evolution of the double core has been investigated for a configuration consisting of a $1 M_{\odot}$ main-sequence star and a $5 M_{\odot}$ red giant in its hydrogen and helium shell burning stage. We have followed the common envelope evolution to the late stages and have demonstrated that more than about $3 M_{\odot}$ can be ejected in an equatorial outflow. This result is insensitive to the binary orbital period immediately prior to the double-core phase (i.e., to the evolutionary state of the red giant). For our choice of model parameters the results were found to be independent of the initial orbital separations from which the hydrodynamical calculations were begun and of the form of the energy dissipation rate. Since the time scale for the orbit to decay is always much greater than the mass-loss time scale during the late stages of double-core evolution in the cases studied here, it is likely that the entire common envelope will be ejected and that the coalescence of the two cores can be avoided. Furthermore, the mass-loss process is found to be adiabatic, but with an efficiency for conversion of orbital energy into mass ejection ranging between 0.3 and 0.6. The incomplete conversion of the energy lost from the orbit to unbind the envelope is due to the nonspherical nature of the ejection process. Consequently, the matter which is ejected is given more than the escape velocity.

Although the mass loss promoted by the double-core evolution is confined primarily to a half-angle of about 13° from the equatorial plane, the mass ejection may take place over a greater angular extent because the outer layers of the very evolved red giants are characterized by positive energies. If nonadiabatic effects are unimportant, then the energy associated with the recombination of helium and hydrogen may facilitate mass loss from other regions away from the equatorial plane as well. Studies of this phase are important and are planned for the future.

Finally, in order to provide a better understanding of the termination of the common envelope phase, we plan to extend our calculations to the late phases to investigate the question of whether circulation-induced mixing in the core region significantly influences the behavior of the hydrogen and helium shell burning regions.

This work was supported in part by the National Science Foundation under grant AST-8608291. The numerical calculations were performed at the National Center for Supercomputing Applications in Urbana, Illinois.

REFERENCES

- Black, D. C., and Bodenheimer, P. 1975, *Ap. J.*, **199**, 619.
 Bodenheimer, P., and Taam, R. E. 1984, *Ap. J.*, **280**, 771 (Paper I).
 ———. 1986, in *The Evolution of Galactic X-Ray Binaries*, ed. J. Trümper, W. H. G. Lewin, and W. Brinkmann (Dordrecht: Reidel), p. 13.
 Bondi, H. 1952, *M.N.R.A.S.*, **112**, 195.
 Counselman, C. C. 1973, *Ap. J.*, **180**, 307.
 Delgado, A. J. 1980, *Astr. Ap.*, **87**, 343.
 Dodd, K. N., and McCrea, W. H. 1952, *M.N.R.A.S.*, **112**, 205.
 Eggleton, P. P. 1971, *M.N.R.A.S.*, **151**, 351.
 ———. 1972, *M.N.R.A.S.*, **156**, 361.
 Flannery, B., and Ulrich, R. 1977, *Ap. J.*, **212**, 533.
 Hoyle, F., and Lyttleton, R. A. 1939, *Proc. Cambridge Phil. Soc.*, **35**, 405.
 Iben, I., Jr., and Tutukov, A. V. 1984, *Ap. J. Suppl.*, **54**, 335.
 Kato, M. 1982, *Pub. Astr. Soc. Japan*, **34**, 173.
 Livio, M., and Soker, N. 1984a, *M.N.R.A.S.*, **208**, 763.
 ———. 1984b, *M.N.R.A.S.*, **208**, 783.
 ———. 1988, *Ap. J.*, **329**, 764.
 Meyer, F., and Meyer-Hofmeister, E. 1979, *Astr. Ap.*, **78**, 167.
 Nariai, K., and Sugimoto, D. 1976, *Pub. Astr. Soc. Japan*, **28**, 593.
 Paczyński, B. 1976, in *IAU Symposium 73, The Structure and Evolution of Close Binary Systems*, ed. P. Eggleton, S. Mitton, and J. Whelan (Dordrecht: Reidel), p. 75.
 Paczyński, B., and Sienkiewicz, R. 1972, *Acta Astr.*, **22**, 73.
 Ritter, H. 1976, *M.N.R.A.S.*, **175**, 279.
 Shima, E., Matsuda, T., Takeda, H., and Sawada, K. 1985, *M.N.R.A.S.*, **217**, 367.
 Shu, F. H., Lubow, S. H., and Anderson, L. 1979, *Ap. J.*, **229**, 223.
 Soker, N., Harpaz, A., and Livio, M. 1984, *M.N.R.A.S.*, **210**, 189.
 Taam, R. E. 1979, *Ap. Letters*, **20**, 29.
 ———. 1988, in *Critical Observations vs. Physical Models for Close Binary Systems*, ed. K. C. Leung (New York: Gordon & Breach), p. 365.
 Taam, R. E., Bodenheimer, P., and Ostriker, J. P. 1978, *Ap. J.*, **222**, 269.
 van den Heuvel, E. P. J., and Taam, R. E. 1984, *Nature*, **309**, 235.
 Verbunt, F. 1987, *Ap. J. (Letters)*, **312**, L23.
 Webbink, R. F. 1976, *Ap. J. Suppl.*, **32**, 583.
 ———. 1977, *Ap. J.*, **211**, 486.

PETER BODENHEIMER: Lick Observatory, University of California, Santa Cruz, CA 95064

RONALD E. TAAM: Department of Physics and Astronomy, Northwestern University, Evanston, IL 60208